



## Hydrodynamic design and performance testing of Pelton-type energy recovery turbine for pressure-retarded osmosis systems

Joo Hoon Park<sup>a,b</sup>, Young Soo Kim<sup>a,b</sup>, In Hyuk Jung<sup>a,b</sup>, Youhwan Shin<sup>b,\*</sup>, Jin Taek Chung<sup>c</sup>

<sup>a</sup>Graduate School of Korea University, Innovation Hall 332, Korea University, Anam-ro 145, Seongbuk-gu, Seoul 02841, Korea, emails: joochoon82@korea.ac.kr (J.H. Park), cusia2002@korea.ac.kr (Y.S. Kim), dlsgur1820@korea.ac.kr (I.H. Jung)

<sup>b</sup>Center for Urban Energy Research, Korea Institute of Science and Technology, Hwarangno 14-gil 5, Seongbuk-gu, Seoul 02792, Korea, email: yhshin@kist.re.kr

<sup>c</sup>Department of Mechanical Engineering, Korea University, Innovation Hall 310, Anam-ro 145, Seongbuk-gu, Seoul 02841, Korea, email: jchung@korea.ac.kr

Received 27 August 2017; Accepted 28 October 2017

---

### ABSTRACT

In this paper, we present the hydrodynamic design and performance tests of a Pelton-type energy recovery turbine (ERT) for pressure-retarded osmosis (PRO) systems. We describe the process of selecting the appropriate type of ERT for operating conditions of the PRO system (i.e., 400 ton/day, 30 bar) as well as the design methods for the Pelton-type ERT. Furthermore, we analyse the performance characteristics at design and off-design points and the change in performance with respect to the diameter of the Pelton runner, based on the performance tests of the manufactured Pelton-type ERT. At the design point, the efficiency of the Pelton-type ERT was approximately 85%, and the overall efficiency with the electric generator was approximately 77.2%. The efficiency of the turbine and overall plant was highest when the diameter of the Pelton runner is of the size selected during design. We thus validate the design result through such a performance test. It is expected that this study will be of great assistance to future works involving the selection of ERTs for PRO systems, as well as the design and performance tests of ERTs.

*Keywords:* Pressure-retarded osmosis; Energy recovery device; Hydrodynamic design of Pelton turbine; Performance test; Production of electric power

---

### 1. Introduction

Seawater desalination, which produces freshwater by removing various solutes in seawater (e.g., salts), is a water processing method that is currently applied to secure alternative water resources to solve the global issue of water deficiency. Seawater desalination based on reverse osmosis (RO) is one of the most common desalination techniques. Recently, osmotic power generation using the concentrate from either seawater or a desalination plant has been highlighted as a future regenerative energy source. There are two types of osmotic power generation that are capable of continuous power generation in a small-scale area: reverse

electro-dialysis and pressure-retarded osmosis (PRO). The two processes utilise osmosis through a membrane. In particular, PRO generates energy by turning the turbine with the pressure energy from the osmosis of the concentrate at a membrane, as shown in Fig. 1.

The first practical conception of PRO was in 1954 [1], when Sidney Loeb harvested the electromotive force of osmosis between seawater and freshwater through a membrane. He devised a PRO power generation method based on the use of osmotic pressure difference between the Jordan River and the Dead Sea. He further developed the theoretical framework, and manufactured a membrane for experimental verification [2–5]. Thereafter, prototype PRO plant designs

---

\* Corresponding author.

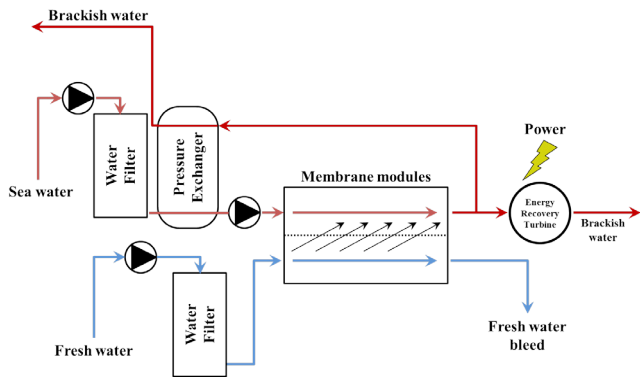


Fig. 1. General schematic diagram of pressure-retarded osmosis system.

and manufacturing projects were conducted worldwide based on technological advances in membrane modules. A Norwegian national power company, Statkraft [6,7], manufactured the first PRO plant for test runs using seawater and freshwater. In Japan, a pilot plant using brine from RO process was operated as part of the Mega-ton project [8]. In Korea, the seawater RO (SWRO)/PRO project is currently in progress, which uses the brine from the SWRO process as the draw solution for PRO. In this regard, Jo et al. [9] analysed jet quality according to the internal angle of the nozzle used in the energy-recovery Pelton turbine through experimental and numerical study.

In a PRO system, an energy recovery device (ERD) or energy recovery turbine (ERT) allows the retrieval of the pressure energy of the concentrate generated by the membrane. Depending on the energy transfer mechanism, ERDs are categorised as either positive-displacement or centrifugal types. While there is a persistent research effort for using RO systems with positive-displacement ERDs in commercial products, it is of rare occasion that centrifugal ERDs or ERTs are developed solely for use in PRO systems. This occurs because of the difficulty in selecting the appropriate centrifugal ERD or ERT due to the operating characteristics of a PRO system.

In this paper, we describe the design process of a Pelton-type ERT developed for PRO systems and analyse its performance at design and off-design points using an in-house developed performance test rig.

## 2. Hydrodynamic design process

### 2.1. Type selection

Since ERTs are similar to common hydraulic turbines, the appropriate turbine type for the operating condition of the PRO system can be selected using a dimensionless quantity known as the specific speed ( $n_s$ ). Fig. 2 is a map that allows for the selection of turbine type based on the net head and specific speed, and the specific speed [10] is:

$$n_s = \frac{NQ^{1/2}}{H^{3/4}} \quad (1)$$

where  $N$  is the rotational speed of the ERT (rad/s),  $Q$  is the volumetric flow rate ( $m^3/s$ ) and  $H$  is the net head (m). The net head

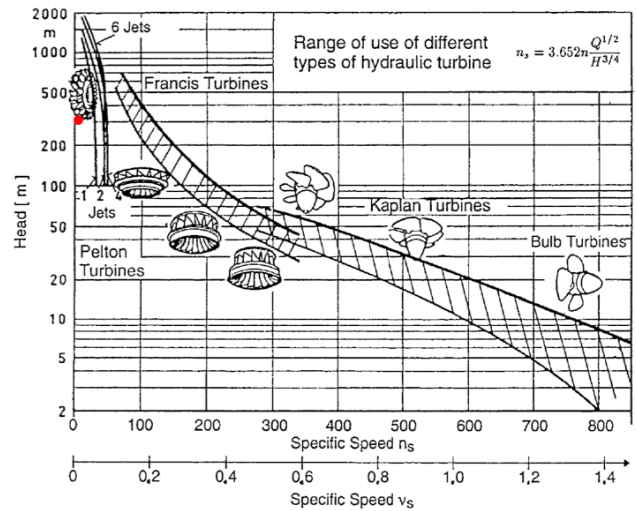


Fig. 2. Selection map of energy recovery turbine type by head vs. specific speed [13].

here refers to the head at the turbine, and in the case of an ERT, the net head can be deduced from the osmosis at the membrane. With the specific speed equation, we can observe the following. If, for example, the net head increases with both flow rate and rotational speed staying constant, the specific speed decreases, and the ERT selection point moves to the left in the map. Meanwhile, if the flow rate increases with both rotational speed and net head staying constant, the ERT selection point moves to the right. Thus, design conditions with higher net head and lower flow rate more likely correspond to Pelton turbines, and those with lower net head and higher flow rate correspond to Kaplan or Bulb turbines. Since the design conditions of the ERT in this study are a flow rate of  $400 m^3/d$ , a net head of 30 bar and a rotational speed of 3,600 rpm (determined in section 2.3), it can be seen from Fig. 2 that the selection point, denoted by the red solid circle, belongs to the region of Pelton turbines.

### 2.2. Design of Pelton-type ERT

Fig. 3 shows the typical shape of a Pelton turbine, which comprises a Pelton runner and spear nozzle. The concentrate extracted from the PRO membrane is injected through the nozzle into the jet, which collides with the Pelton bucket. Since the kinetic energy received by the bucket rotates the Pelton runner to generate electricity, the design of the nozzle and Pelton runner in an ERT is critically important. The design of the Pelton-type ERT was based on computing the main design variables with reference to the process and methods previously used in the design of Pelton turbines for hydroelectric generators [11–13]. There are four main design variables for a Pelton runner: the jet velocity  $v_{jet}$ , jet diameter  $d_{jet}$ , runner diameter (i.e., pitch circle diameter—PCD) and runner rotational speed  $N$ .

The velocity of the jet is determined by:

$$v_{jet} = C_v \sqrt{2gH} \quad (2)$$

where  $C_v$  is the velocity coefficient,  $g$  is the gravitational acceleration and  $H$  is the net head. While the velocity coefficient

varies with the shape of the nozzle, the value of 0.97 was used in this study as it is commonly used for spear nozzles [11]. The net head was chosen based on the pressure generated by the PRO membrane.

The jet diameter is calculated based on the operating flow rate, the velocity of the jet and the number of nozzles:

$$d_{\text{jet}} = \sqrt{\frac{4Q}{\pi v_{\text{jet}} n_{\text{jet}}}} \quad (3)$$

The number of nozzles,  $n_{\text{jet}}$ , can range from one to six depending on the operating flow rate [11]. In this study, only one nozzle was used owing to considerations of the operating flow rate and jet diameter.

The rotational speed of the runner is calculated from the speed ratio  $x$ , PCD and the jet velocity:

$$N = \frac{60x}{\pi \text{PCD}} v_{\text{jet}} \left( \ast x = \frac{v_{\text{tan,pcd}}}{v_{\text{jet}}} \right) \quad (4)$$

The speed ratio  $x$  in Eq. (4) is given by the ratio between the tangential velocity at the PCD and the velocity of the jet. According to previous research [11], while the theoretical speed ratio for optimal efficiency is 0.5, the efficiency is optimal when the speed ratio is, in fact, 0.46 when losses are taken into account. Thus, in this study, a speed ratio of 0.46 was used as the design constraint.

### 2.3. Matching rotational speed and Pelton runner diameter

The rotational speed of a generator is given in terms of the scheduled frequency  $f$  and the number of poles  $Z_p$ :

$$N = 120 f / Z_p \quad (5)$$

Since the scheduled frequency is fixed at 60 Hz in Korea, the rotational speed can be determined from the number of poles in the generator. Typically, the number of poles in a generator increases in multiples of two, and the rotational speed

decreases with an increasing number of poles. However, the diameter of the Pelton runner increases with decreasing rotational speed, increasing the weight and manufacturing cost; thus, an appropriate rotational speed must be chosen. In this study, the rotational speed of the Pelton runner was chosen as 3,600 rpm, which is the rotational speed of an induction generator that rotates in accordance with the scheduled frequency.

### 2.4. Design results of Pelton runner

The aforementioned rotational speed, PCD, jet velocity and speed ratio are crucial parameters in the design of a Pelton runner. Furthermore, the Pelton bucket can be designed based on these design variables. A Pelton bucket is mainly affected by the jet diameter, with which the shape and size of the bucket varies. Previous works [11–13] proposed numerous equations and methods for the selection of the shape of the Pelton bucket. In this paper, we designed the bucket based on the shape suggested by Thake [11], and Table 1 shows the results of the one-dimensional design of the Pelton turbine. Fig. 4 shows the three-dimensional shape of the Thake-type bucket, which was designed based on the one-dimensional design, as well as the assembled Pelton runner.

### 2.5. Manufacture of Pelton-type ERT

Fig. 5 shows the Pelton bucket and a spear nozzle that can control the flow rate and pressure, which were machined using a 5-axis lathe machine. A stepper motor was installed at one end of the spear nozzle, so that the needle inside the nozzle could be controlled. All components of the Pelton-type ERT, including the spear nozzle, Pelton runner, axis and casing, were made of stainless steel 316L. This material was selected based on considerations of accessibility, ease of machining and corrosion resistance.

## 3. Description of performance test setup

Fig. 6 shows a diagram of the performance test rig for the Pelton-type ERT used in this study. The working fluid of the performance test rig is water, which circulates in a closed loop where it passes through a high-pressure pump, accelerates through the spear nozzle and returns to the water tank. A bypass line was installed in the middle of the pipe to control

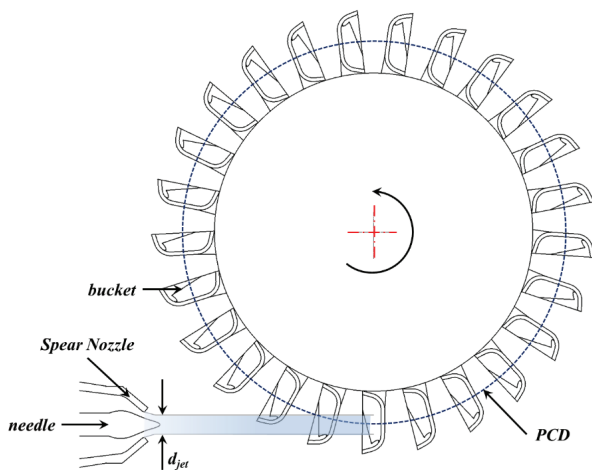


Fig. 3. General structure of Pelton runner and spear nozzle.

Table 1  
Preliminary hydrodynamic design results of Pelton-type ERT

Design parameter	Design result value
Volume flow rate, LPM	277.8
Net head, m	300
Velocity from nozzle, m/s	74.4
Number of nozzles	1
Diameter of jet, mm	9
Pitch circle diameter, mm	182
Rotation speed, rpm	3,600
Number of buckets	25

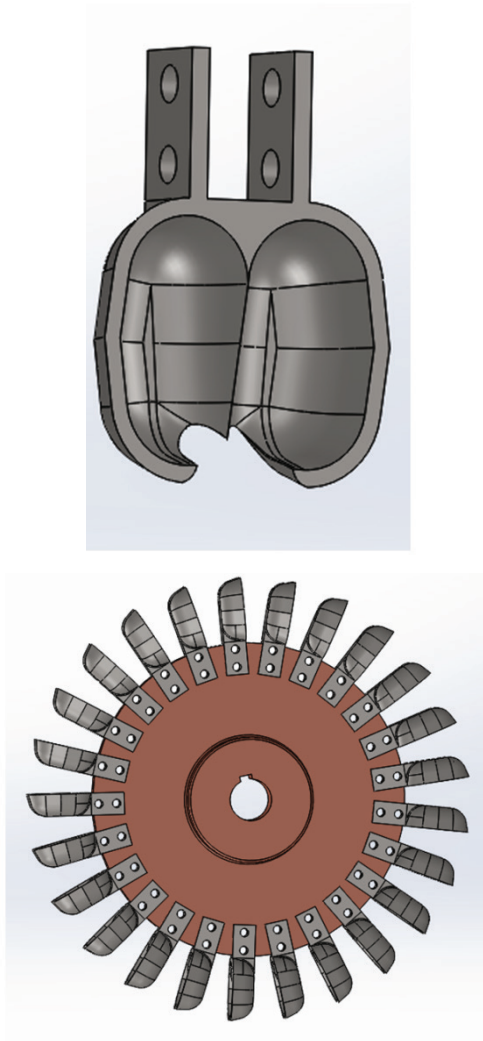


Fig. 4. Three-dimensional design of Pelton bucket and assembled Pelton runner.



Fig. 5. Manufactured Pelton bucket and spear nozzle.

the flow rate while maintaining the pressure. A flow meter was installed in the main pipe, and a pressure transducer and a pressure gauge were installed near the spear valve. A torque transducer was installed between the Pelton turbine

and the generator shaft. A proximity sensor was installed on one side of the generator shaft, and the output power of the generator was measured using a power meter. The system was configured to monitor and save in real-time all electrical signals from the flow meter, pressure transducer, torque transducer and power meter.

The performance test of the ERT was conducted by fixing the operating pressure at 30 bar, and gradually decreasing the flow rate in equal increments. Moreover, since the induction generator cannot operate at rotational speeds lower than 3,600 rpm, the performance test ended when the manipulation of the flow rate resulted into a rotational speed near 3,600 rpm. Fig. 7 depicts the performance test rig and the assembled Pelton-type ERT.

#### 4. Results and discussion

##### 4.1. Performance of Pelton-type ERT with varying flow conditions

Following are the performance characteristics at the design and off-design points of the Pelton turbine. The operating flow rate and net head were nondimensionalised [14] using the flow rate parameter ( $\Phi$ ) and the net head parameter ( $\Psi$ ) in order to evaluate the efficiency of the ERT ( $\eta_{ERT}$ ):

$$\Phi = \frac{Q}{\pi R^3 \omega} \tag{6}$$

$$\Psi = \frac{2gH}{R^2 \omega^2} \tag{7}$$

$$\eta_{ERT} = \frac{\text{Turbine shaft power}}{\text{Input power}} = \frac{T\omega}{\rho gQH} \tag{8}$$

Here  $Q$  is the measured flow rate,  $H$  is the head measured before the nozzle,  $R$  is the radius of the Pelton runner (i.e.,  $R = \text{PCD}/2$ ),  $\omega$  is the angular velocity of the runner (i.e.,  $\omega = N/2\pi$ ),  $g$  is gravitational acceleration (density of water at 25°C, = 997 kg/m<sup>3</sup>) and  $T$  is the measured torque used to compute the efficiency of the ERT.

Fig. 8 shows a comparison of the efficiency of the ERT and shaft output power, and Fig. 9 shows a comparison of the net efficiency, including the ERT efficiency and the generator efficiency, and the generator output power. The output power with varying flow rate was measured for nozzle pressures (i.e., 15, 20, 25 and 30 bar). Qualitative trends were analysed by fitting polynomial curves to the efficiencies (solid symbol and line) and by fitting linear curves to the output power of turbine shaft and generator (open symbol and dash line).

The net efficiency in Fig. 9 is smaller than the efficiency of turbine alone (Fig. 8), since the efficiencies of the turbine and generator are combined. Examining the trend in net and turbine efficiency, the efficiency slowly decreases with decreasing flow rate at a rate of 2–3%, yet an abrupt decrease in efficiency occurs below a certain flow rate. This results from multiple causes. First, to reduce the flow rate, the needle for pressure control moves toward the nozzle exit, which reduces the jet diameter, so the cross sectional area hitting the bucket decreases. Second, even at constant pressure, the shaft torque decreases along with the reduction in fluid energy received by the bucket as the operating flow rate decreases. Third,

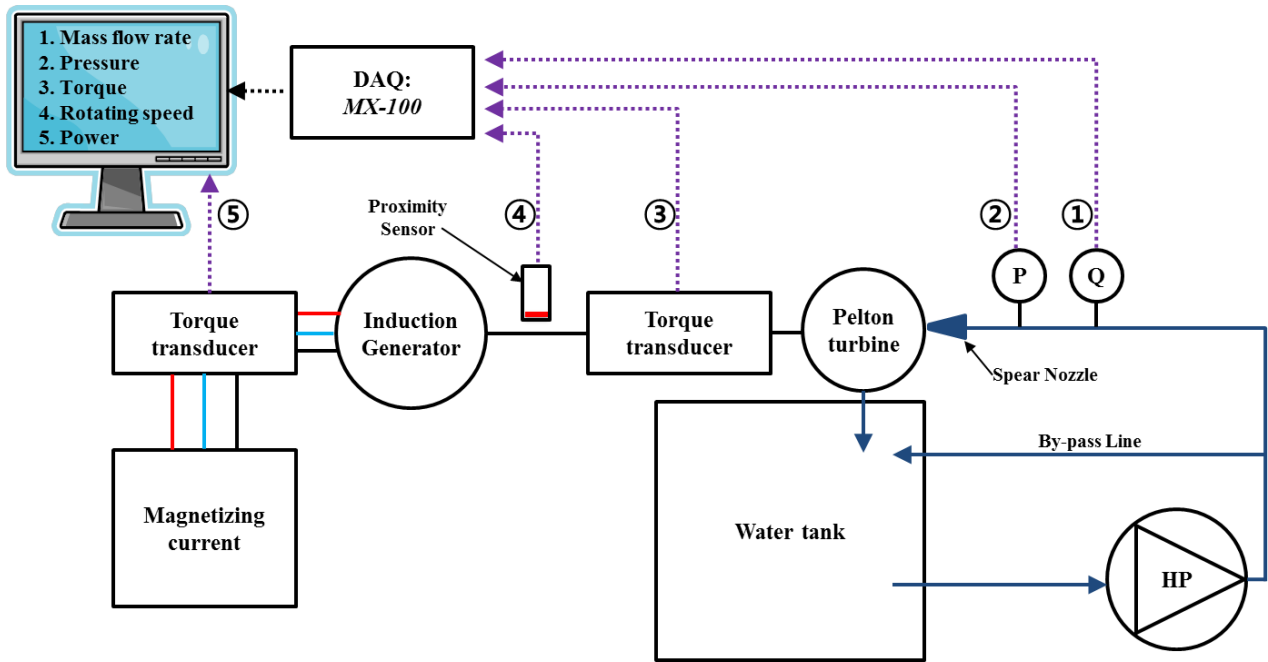


Fig. 6. Schematic diagram of performance test for Pelton-type ERT.

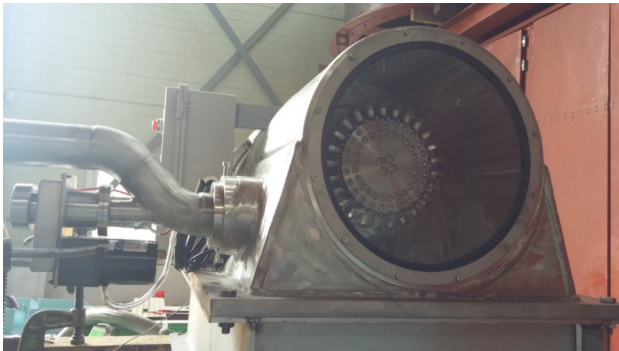


Fig. 7. Assembled performance test rig with Pelton-type ERT.

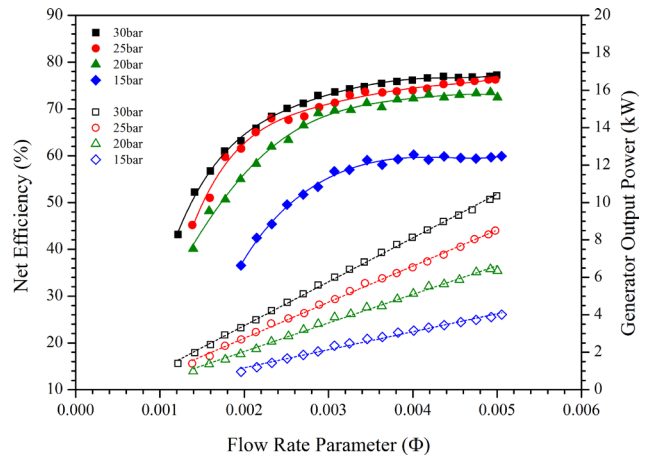


Fig. 9. Comparison of net efficiency and generator output power for various flow rates.

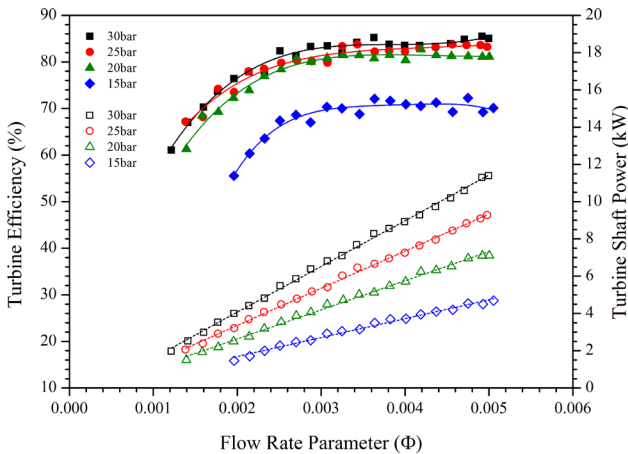


Fig. 8. Comparison of ERT efficiency and shaft power for various flow rates.

it appears that the relative effect of hydraulic loss (e.g., friction loss in the bucket, friction loss of bearings and windage loss) increases. The rotational speed was maintained within a variation of approximately 1% during operation, so it is believed that it had no significant effect.

Additionally, the net and turbine efficiencies are highest when the nozzle pressure is at 30 bar for all flow rates considered. Moreover, if the nozzle pressure decreases, the efficiency decreases since the torque decreases with the reduction in input power. However, if the nozzle pressure drops down to 15 bar, the turbine efficiency decreases by approximately 15%p and the net efficiency by 18%p compared with the design flow rate. Table 2 presents the quantitative description of the turbine and net efficiencies and the speed ratio. The table shows that the speed ratio at 30 bar

Table 2  
Comparison of speed ratio and efficiency at design flow rate

Inlet pressure of nozzle (bar)	ERT efficiency (%)	Net efficiency (%)	Speed ratio
30	85	77	0.46
25	83	76	0.51
20	81	72	0.57
15	70	59	0.65

is approximately 0.46, which corresponds to the maximum efficiency point proposed by previous research [11]. If the nozzle pressure decreases, the jet velocity decreases; thus, the speed ratio increases inversely proportional to this. If the speed ratio increases, the efficiency decreases owing to the increase in windage, friction loss and water-missing [11], where the energy of the jet is not delivered to the bucket. Thake [11] has described that if the speed ratio is more than 0.6, performance degradation is known to occur because of missing flow. Missing flow dramatically increase when the Pelton wheel is much faster than the jet velocity. It means that the considerable flow does not transfer energy to the bucket. Therefore, the efficiency difference between 15 and 30 bar is greater than other operating pressure conditions (Fig. 10). It is determined the missing flow has a dominant influence.

The results shown in Figs. 8 and 9 validate that the output power is a function of the flow rate and pressure, as the shaft and generator output powers of the turbine increase linearly with the increase in flow rate and nozzle pressure.

Fig. 11 shows a contour plot of the efficiency of the ERT with respect to the change in flow rate parameter and net head parameter. Solid lines represent changes in the net head parameter with the changes in the flow rate parameter for each of the sample groups between 15 and 30 bar. While the pressure was fixed and the performance test was conducted for the change in flow rate, Eqs. (6) and (7) show that the net head parameter decreases with increasing flow rate parameter owing to the effect of rotational speed. It can also be observed that the ERT efficiency increases along with flow rate and net head as in Fig. 8, and that the region with 80% efficiency or higher becomes wider above 20 bar. We verified that at the design point (400 ton/d, 30 bar) the efficiency of the Pelton-type ERT is 85%, and that the net efficiency including generator is 77%.

4.2. Performance of ERT with respect to PCD

In this section, we present comparisons of the performances of the ERT and entire plant for various diameters of the Pelton runner. The Pelton runner is the most important component in the Pelton-type ERT, which operates the generator by receiving the pressure energy of the concentrate. In particular, the PCD of the Pelton runner is one of the most important design variables, as it is related to performance characteristics, such as shaft output power and efficiency, through the speed ratio.

Fig. 12 compares three values for the PCD (178, 182, and 185.9 mm) in terms of ERT efficiency and shaft output power with respect to input power for identical nozzle inlet

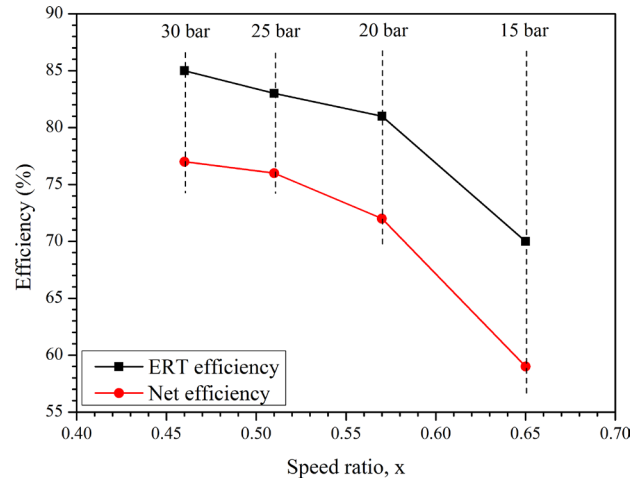


Fig. 10. Comparison of ERT and net efficiencies by speed ratio at each inlet nozzle pressure.

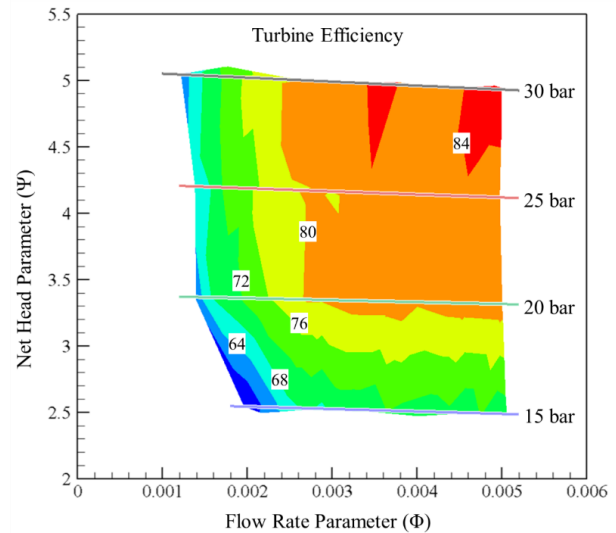


Fig. 11. Efficiency contours of ERT.

pressures. Here, input power refers to the energy of the jet injected from the nozzle. Figs. 12(a) and (b) are the performance maps for 20 and 30 bar nozzle pressures, respectively. From Figs. 12(a) and (b), the output power of the turbine increases linearly with the input power, and the turbine shaft output power is very similar for each PCD when the nozzle pressure is at 20 bar. In terms of turbine efficiency, while a PCD of 178 mm is greatest for input powers below 4.7 kW, all runners become identical when input power is raised. We believe that the high efficiency occurs for the PCD of 178 mm at input powers below 4.7 kW because of its lower weight compared with runners with larger PCDs, which decreases friction loss. While it was predicted that the output of PCD 178 mm would produce less torque owing to its smaller radius, the analysis showed that the torque was equivalent to the other PCDs owing to the efficiency gains due to lower weight.

Fig. 12(b) shows that a PCD of 178 mm is lower than PCDs of 182 and 185.9 mm in terms of both output and efficiency

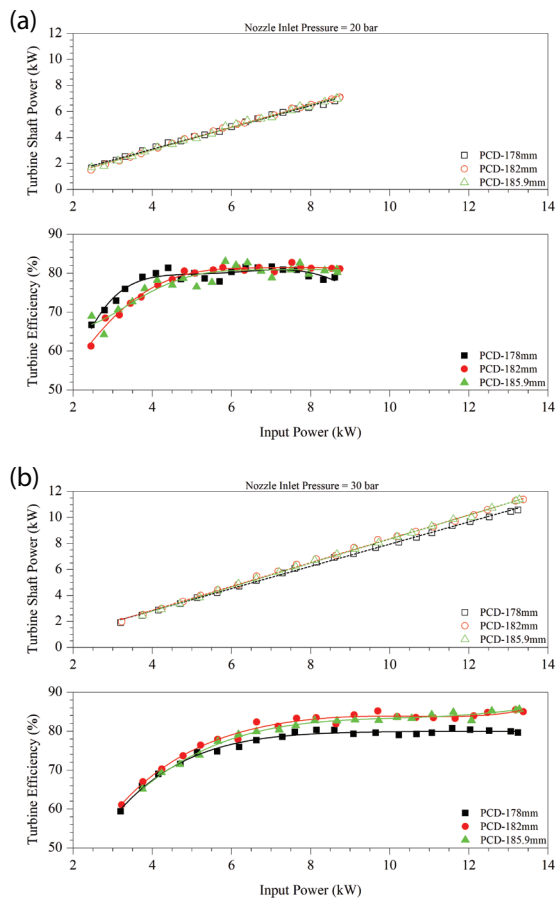


Fig. 12. Comparison of ERT efficiency and turbine shaft power for different Pelton runner diameters at constant nozzle inlet pressure. (a) Nozzle inlet pressure = 20 bar and (b) Nozzle inlet pressure = 30 bar.

even if the nozzle pressure increases. While the shaft output power and trend in efficiency for PCDs of 182 and 185.9 mm are mostly identical, the shaft output power of a PCD of 182 mm is 1.1% greater than that of a PCD of 185.9 mm, and the efficiency is 0.2–2% greater.

Figs. 13(a) and (b) compare the performance when the nozzle pressure is at 20 and 30 bar, respectively. The trend in generator output power at a nozzle entrance pressure of 20 bar shown in Fig. 13(a) is similar to the trend in the turbine output power as seen in Fig. 12(a). However, while the PCD of 178 mm is again more efficient for input powers less than 4.7 kW, the efficiency at a PCD of 182 mm is higher for input powers greater than 4.7 kW. Furthermore, Fig. 13(b) shows that the PCD of 182 mm is greatest in terms of net efficiency and output power at nozzle entrance pressures of 30 bar.

Theoretically, for the same rotational speed, the shaft output power of a turbine increases with the increasing PCD of the runner. However, analysis showed that a PCD of 182 mm is more efficient than 185.9 mm as the increase in PCD entails an increase in weight of the runner and thereby additional mechanical friction loss. Therefore, considering total efficiency, weight and manufacturing costs, 182 mm is considered the most appropriate PCD.

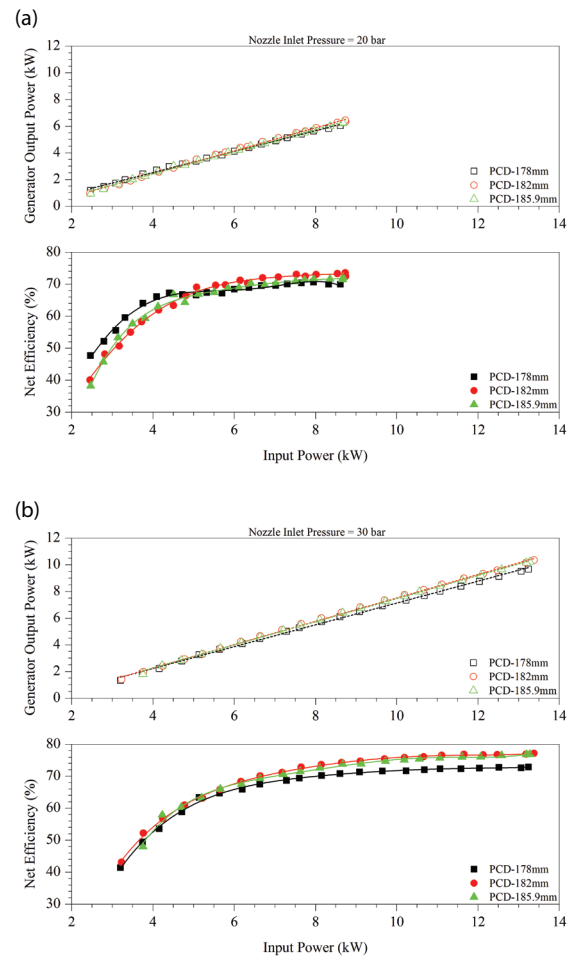


Fig. 13. Comparison of net efficiency and generator output power for different Pelton runner diameter at constant nozzle inlet pressures. (a) Nozzle inlet pressure = 20 bar and (b) nozzle inlet pressure = 30 bar.

### 5. Conclusion

In this paper, we presented the hydrodynamic design process and performance characteristics of a Pelton-type ERT for use with PRO systems. The hydrodynamic design method and results for the Pelton-type ERT were validated through performance tests at the design point. The efficiency of the manufactured Pelton-type ERT is approximately 85% and total efficiency including an electric generator is approximately 77%, generating about 10.4 kW output power. Moreover, we confirmed that the efficiency is the highest at a speed ratio of 0.46. We obtained the operating region and performance characteristics of the Pelton-type ERT through performance tests at off-design points, and observed that the output power and efficiency are the highest at the design result of a PCD of 182 mm through a performance test in which the PCD was varied. This confirms that the PCD is an important design factor that affects the performance of an ERT, and furthermore validates the design results. It is expected that the presented ERT selection process, design method and performance test method will significantly assist future research into Pelton-type ERTs for PRO systems.

### Acknowledgement

This research was supported by a grant (code 17IFIP-B065893-05) from the Industrial Facilities & Infrastructure Research Program funded by Ministry of Land, Infrastructure and Transport of the Korean government.

### References

- [1] R.E. Pattle, Production of electric power by mixing fresh and salt water in the hydroelectric pile, *Nature*, 174 (1954) 660.
- [2] S. Loeb, Method and Apparatus for Generating Power Utilizing Pressure-Retarded-Osmosis, Israel Patent Application 42658 (July 3, 1973), United States Patent 3906250 (Sep 16, 1975).
- [3] S. Loeb, R.S. Norman, Osmotic power plants, *Science*, 189 (1975) 654–655.
- [4] S. Loeb, F.V. Hessen, D. Shahaf, Production of energy from concentrated brines by pressure-retarded osmosis: II. Experimental results and projected energy costs, *J. Membr. Sci.*, 1 (1976) 249–269.
- [5] S. Loeb, Energy production at the Dead Sea by pressure-retarded osmosis: challenge or chimera?, *Desalination*, 120 (1998) 247–262.
- [6] S.E. Skilhagen, J.E. Dugstad, R.J. Aaberg, Osmotic power—power production on the osmotic pressure difference between waters with varying salt gradients, *Desalination*, 220 (2008) 476–482.
- [7] K. Gerstandt, K.V. Peinemann, S.E. Skilhagen, T. Thorsen, T. Holt, Membrane processes in energy supply for an osmotic power plant, *Desalination*, 224 (2008) 64–70.
- [8] N. Kishizawa, K. Tsuzuki, M. Hayatsu, Low pressure multi-stage RO system developed in “Mega-ton Water System” for large-scaled SWRO plant, *Desalination*, 368 (2015) 81–88.
- [9] I.C. Jo, J.H. Park, J.-W. Kim, Y.H. Shin, J.T. Chung, Jet quality characteristics according to nozzle shape of energy-recovery Pelton turbines in pressure retarded osmosis, *Desal. Wat. Treat.*, 57 (2016) 24626–24635.
- [10] P. Drtina, M. Sallaberger, Hydraulic turbines – basic principles and state-of-the-art computational fluid dynamics applications, *Proc. Inst. Mech. Eng., Part C: J. Mech. Eng. Sci.*, 213 (1999) 85–102.
- [11] J. Thake, *The Micro-hydro Pelton Turbine Manual: Design, Manufacture and Installation for Small-scale Hydro-power*, Practical Action Publishing, Warwickshire, UK, 2000.
- [12] M. Eisenring, *Micro Pelton Turbine—MHPG Series Harnessing Water Power on a Small Scale*, Volume 9, SKAT Publishing, St. Gallen, Switzerland, 1991.
- [13] K. Subramanya, *Hydraulic Machines*, McGraw Hill Education India, New Delhi, India, 2013.
- [14] F.G. Stamatelos, J.S. Anagnostopoulos, D.E. Papantonis, Performance measurements on a Pelton turbine model, *Proc. Inst. Mech. Eng., Part A: J. Power Energy*, 225 (2011) 351–362.